Electronic Supplementary Material (ESI) for Physical Chemistry Chemical Physics.

Enhanced mechano-responsive fluorescence in polydiacetylene thin films through functionalization with tetrazine dyes

Luca Polacchi[a], Arnaud Brosseau[a], Régis Guillot[b], Rémi Métivier[a], Clémence Allain*[a]*

Supporting Information

a. Université Paris-Saclay, ENS Paris-Saclay, CNRS, PPSM, 91190 Gif-sur-Yvette, France

b. Université Paris-Saclay, CNRS, Institut de Chimie Moléculaire et des Matériaux d'Orsay, 91405, Orsay, France

*Corresponding authors' e-mail: clemence.allain@ens-paris-saclay.fr, remi.metivier@ens-paris-saclay.fr

Table of Contents

1. Synthetic protocols

1.1. Hex-5-yn-1-yl propylcarbamate, 3-chloro-6-(dodecyloxy)-1,2,4,5-tetrazine, Butyl(((12-hydroxydodeca-5,7-diyin-1-yl)oxy)carbonyl)glycinate

Hex-5-yn-1-yl propylcarbamate, and **3-chloro-6-(dodecyloxy)-1,2,4,5-tetrazine** have been synthesized following the protocols described in reference 26 of the main text, **Butyl(((12-hydroxydodeca-5,7-diyin-1-yl)oxy)carbonyl)glycinate** has been synthesized following the protocols described in reference 25 of the main text.

1.2. 1-bromo-pentadec-1-yne

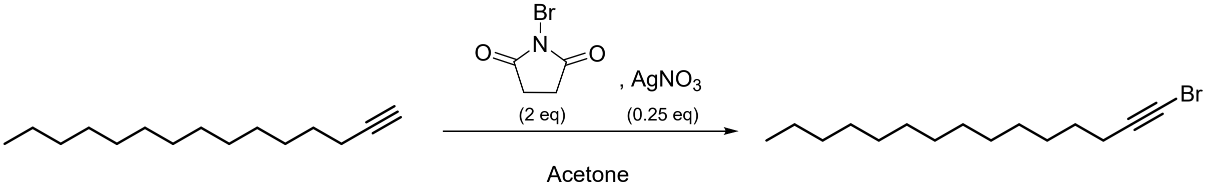

Scheme S1: synthesis of 1-bromo-pentadec-1-yne

In a round bottom flask 0.900 mL (3.43 mmol) of 1-pentadecyne are dissolved in 50 mL of acetone and 1.22 g (6.86 mmol) of N-bromo-succinimmide (NBS) are added to the solution. The solution turns immediately yellow, and a yellow precipitate corresponding to the degradation products of NBS deposits at the bottom of the flask. 0.175 g of silver nitrate $AgNO_3$ are added, the solution turns to milky white and the flask is protected from light with aluminum paper. The mixture is let react for 40 minutes and TLC in petroleum ether shows the complete disappearance of 1-pentadecyne and the appearance of a new spot under UV at 254 nm, corresponding to 1-bromopentadec-1-yne. The reaction mixture is filtered on celite and concentrated on rotavapor. A yellow powder is obtained, due to the presence of residual NBS salts. The powder is dissolved in dichloromethane and filtered on SiO_2 to remove the NBS salts. The solvent is dried to obtain 0.932 g of a yellow-brown oil, (yield = 94.6 %).

^{1}H NMR ($CDCl_3$): δ = 0.88 (3H, t, *J* = 7.0 Hz); 1.26 (20H, m); 1.51 (2H, m); 2.19 (2H, t, *J* = 7.2 Hz) ppm

^{13}C NMR ($CDCl_3$): 80.7, 37.5, 32.1, 29.83, 29.80 (2C), 29.76, 29.6, 29.5, 29.2, 28.9, 28.4, 22.9, 19.8, 14.3 ppm

1.3. DA1

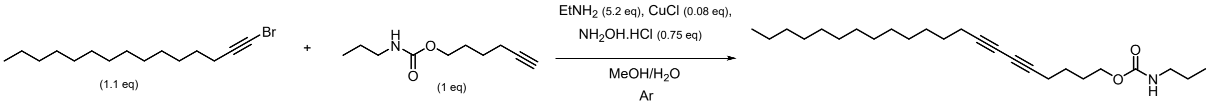

Scheme S2: synthesis of **DA1** by a Cadiot-Chodkiewicz coupling

0.020 g (0.20 mmol) of copper chloride CuCl are introduced in a round bottom flask under argon flux. 0.47 mL of methanol, 1.35 of distilled water and 0.730 mL (1.32 mmol) of ethylamine are added. The solution takes an intense blue color due to the presence of Cu^{2+} ions in solution. 0.132 g (1.90 mmol) of hydroxylamine chloride are added to reduce Cu(II) ions to Cu(I), and the solution color disappears. Under Ar atmosphere, 0.464 g (2.53 mmol) of hex-5-yn-1-yl propylcarbamate are added to obtain a bright yellow solution. 0.800 g (2.78 mmol) of 1-bromopentadec-1-yne are added to the mixture and a foamy blue-green precipitate appears. The reaction mixture is heated to 40°C and let react overnight under stirring. TLC 9:1 petroleum ether/ethyl acetate shows the presence of residual bromopentadecyne and a new spot active in the UV 254 nm corresponding to **DA1**. The reaction solution is diluted with 10 mL of dichloromethane and washed 4 times with 20 mL of NH_4Cl_{sat}. The organic phases are joined, dried on $MgSO_4$ and concentrated. The resulting solid is purified by SiO_2 column chromatography with 9:1 petroleum ether/ethyl acetate, to give 0.724 g of a white powder (yield = 73.5%) that polymerizes very easily under ambient light, giving a blue powder.

^{1}H NMR ($CDCl_3$): δ = 0.90 (6H, m); 1.26 (20H, m); 1.51 (4H, m); 1.59 (2H, m); 1.72 (m, 2H); 2.24 (2H, t, J_1 = 7.2 Hz); 2.30 (2H, t, J_1 = 6.8 Hz); 3.13 (2H, dt, $J_1 = J_2$ = 6.4 Hz); 4.06 (2H, t, J = 6.2 Hz); 4.64 (1H, s) ppm.

^{13}C NMR ($CDCl_3$): 156.8; 78.0; 65.9; 65.3; 64.2; 42.8; 32.1; 29.8; 29.6; 29.5; 29.2; 29.0; 28.5; 28.3; 25.0; 23.4; 22.8; 19.3; 19.1; 14.3; 11.3 ppm.

HRMS (ESI) $[M + H]^+$ calculated = 390.3372; $[M + H]^+$ found = 390.3362;

mp = 74.4°C

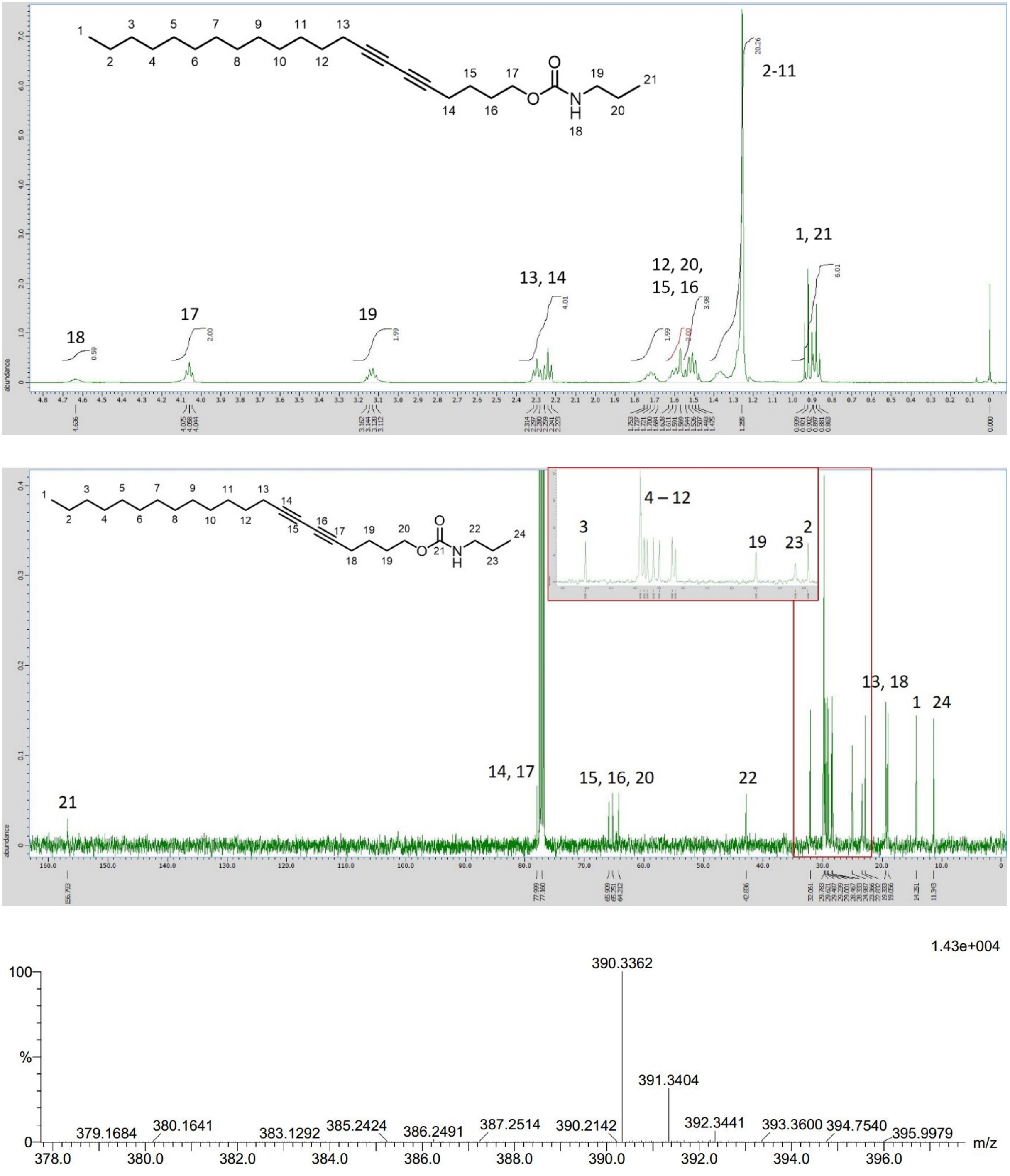

Figure S1: ^{1}H (top) and ^{13}C (middle) NMR spectra of **DA1;** HRMS spectrum (bottom) of **DA1**

1.4. TzDA2

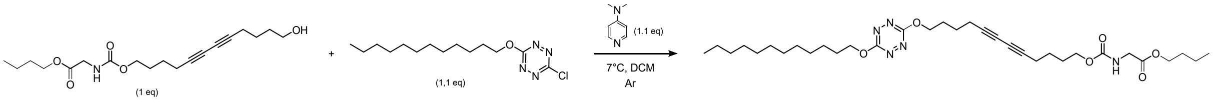

Scheme S3: synthesis of **TzDA2**

0.866 g (2.46 mmol, 1 eq.) of butyl (((12-hydroxydodeca-5,7-diyn-1-yl)oxy)carbonyl) glycinate, 0.814 g (2.71 mmol, 1.1 eq.) of 3-chloro-6-(dodecyloxy)-1,2,4,5-tetrazine and 0.331 g (2.71 mmol, 1.1 eq.) of dimethylaminopyridine (DMAP) are added in a Schlenk, previously dried under vacuum to remove any trace of humidity. The system is brought under nitrogen and 20 mL of dichloromethane are introduced in the flask through a syringe. The reaction is let run under inert atmosphere at 7°C overnight. The product solution is concentrated on rotavapor and purified by SiO_2 column chromatography 8:2 petroleum ether/ethyl acetate to give 0.356 g of **TzDA2** (yield = 24%).

^{1}H NMR ($CDCl_3$): δ = 0.87 (3H, t, J = 6.8 Hz); 0.94 (3H, t, J = 7.0 Hz); 1.26 – 1.37 (16H, m); 1.50 (2H, m); 1.61 (6H, m); 1.75 (4H, m); 1.90 (2H, m); 2.04 (2H, m); 2.30 (2H, t, J = 6.8 Hz); 2.37 (2H, t, J_1 = 7.0 Hz); 3.95 (2H, d, J = 5.2 Hz); 4.10 (2H, t, J = 6.4 Hz); 4.16 (2H, t, J = 6.8 Hz); 4.54 (2H, t, J = 6.4 Hz); 4.57 (2H, t, J = 6.4 Hz); 5.13 (1H, s).

^{13}C NMR ($CDCl_3$): δ = 170.3; 166.3; 166.1; 156.6; 70.2; 69.3; 66.1; 65.8; 65.5; 64.8; 42.8; 32.0; 30.7; 29.8; 29.7; 29.6; 29.5; 29.4; 28.8; 28.2; 27.9; 25.9; 24.8; 24.7; 22.8; 19.2; 19.0; 14.2; 13.8 ppm.

HRMS (ESI) $[M + H]^+$ calculated = 616.4074; $[M + H]^+$ found = 616.4103;

mp = 64.6°C

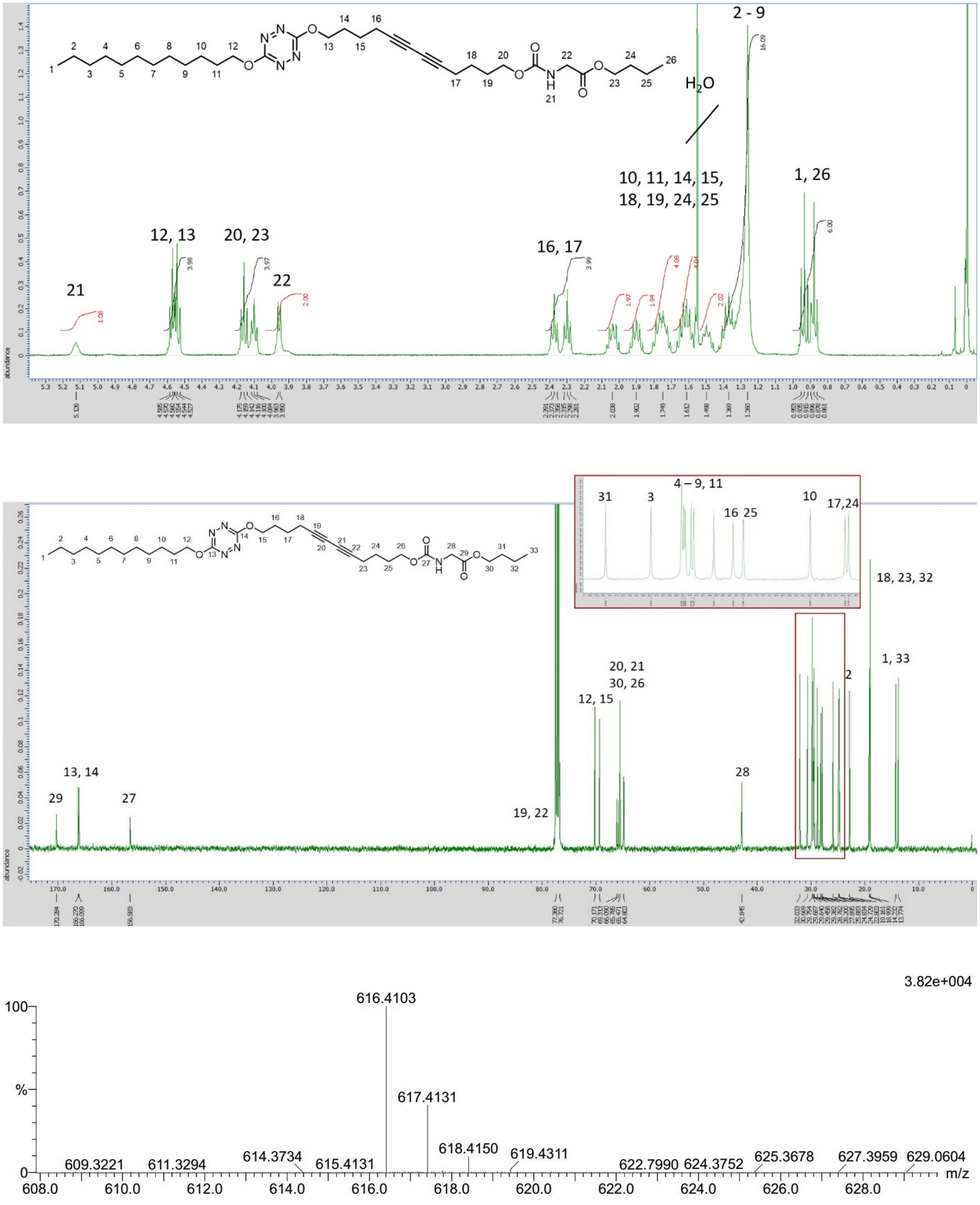

Figure S2: ^{1}H (top) and ^{13}C (middle) NMR spectra of **TzDA2;** HRMS spectrum (bottom) of **TzDA2**

1.5. X-ray structure of TzDA1

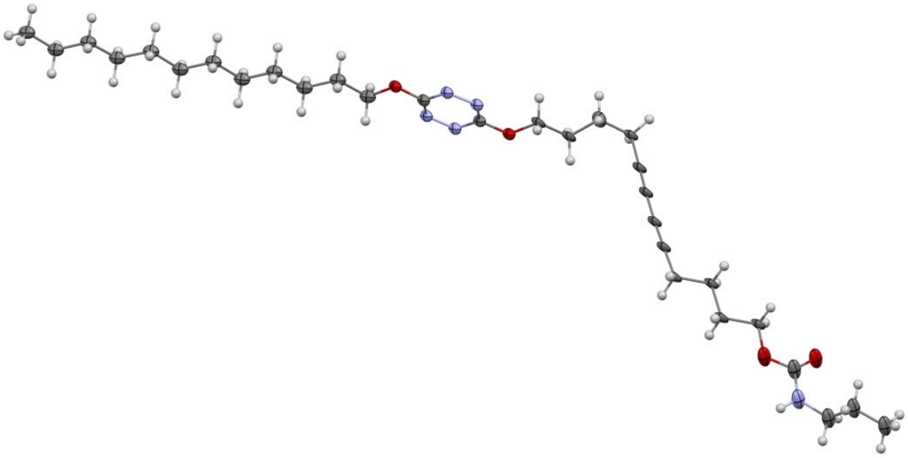

Figure S3. An ORTEP drawing of compound **TzDA1**. Thermal ellipsoids are shown at the 30%.

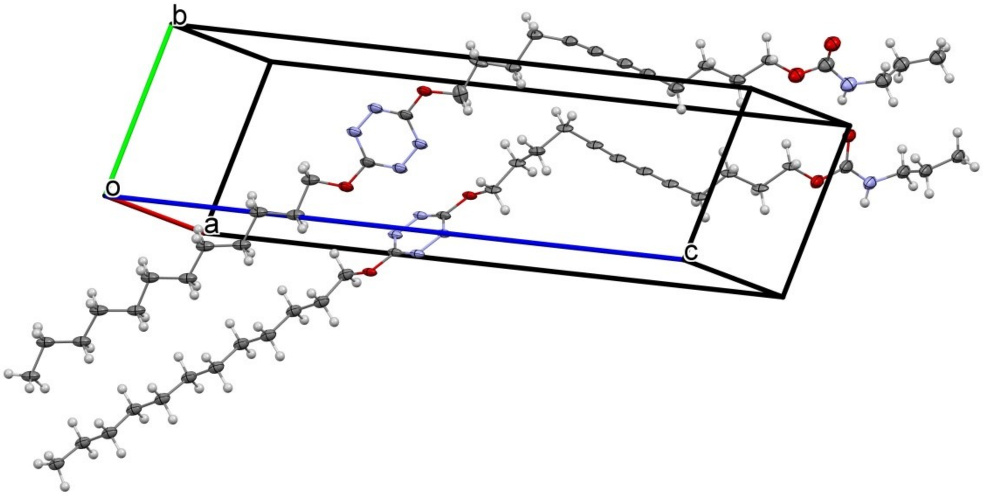

Figure S4. Asymmetric unit of **TzDA1**. Thermal ellipsoids are shown at the 30%.

As displayed in Figure S4, there are two molecules in the asymmetric unit.

CCDC 2010463 contains the supplementary crystallographic data for this paper. These data can be obtained free of charge from the Cambridge Crystallographic Data Centre via http://www.ccdc.cam.ac.uk/Community/Requestastructure.

Table S1. Crystallographic data and structure refinement details.

Compound	**TzDA1**
CCDC	2010463
Empirical Formula	$C_{30} H_{49} N_5 O_4$
M_r	543.74
Crystal size, mm^3	0.010 x 0.030 x 0.040
Crystal system	triclinic
Space group	*P* 1
a, Å	7.1986(18)
b, Å	7.5910(18)
c, Å	28.718(7)
α, °	84.702(17)
β, °	89.324(18)
γ, °	80.32(2)
Cell volume, Å^3	1540.4(7)
Z ; Z’	2 ; 2
T, K	100 (1)
Radiation type ; wavelength Å	CuKα; 1.54178
F_{000}	592
μ, mm^{-1}	0.625
range, °	3.091 - 59.739
Reflection collected	11 010
Reflections unique	7 342
R_{int}	0.2487
GOF	0.984
Refl. obs. (I>2(I))	1 932
Parameters	306
wR_2 (all data)	0.3950
R value (I>2(I))	0.1715
Largest diff. peak and hole (e-.Å^{-3})	0.327 ; -0.298

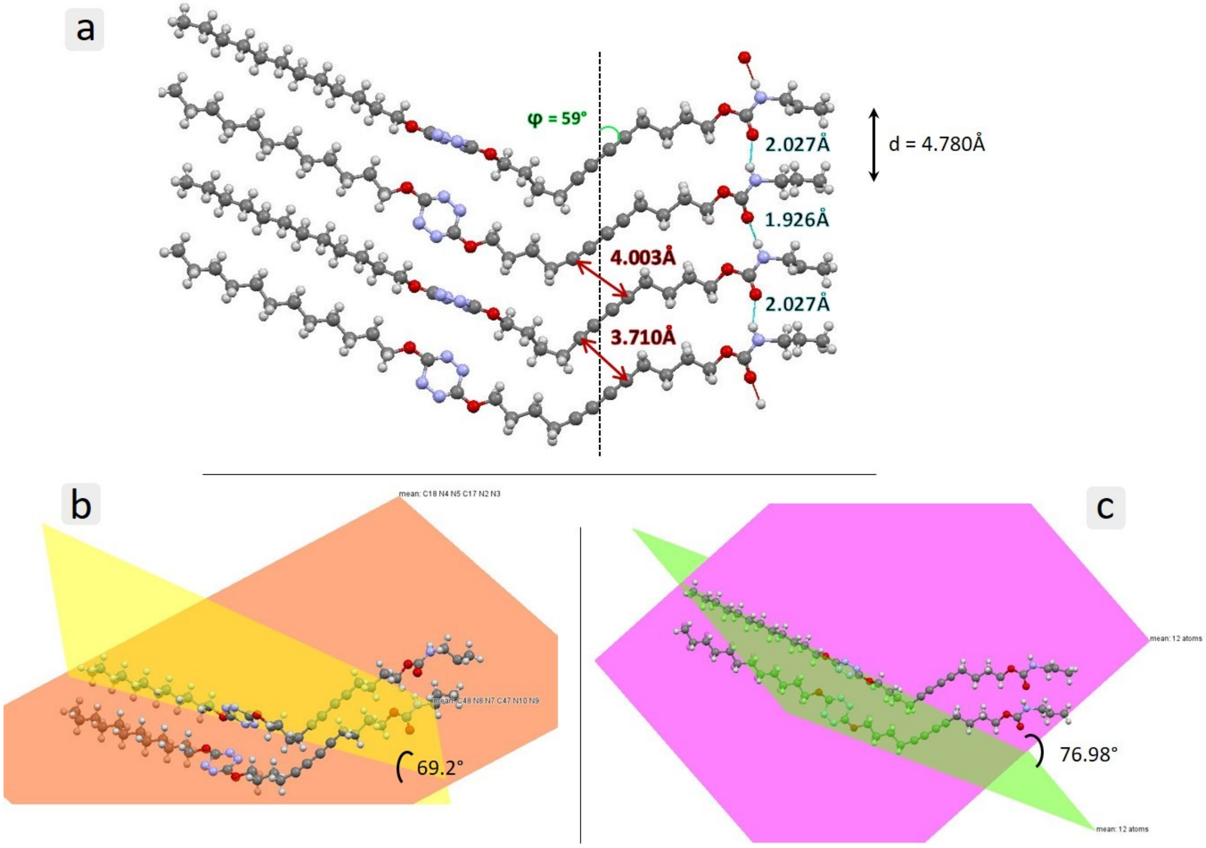

Figure S5. X-ray structure of **TzDA1**. Figure **a** shows the key distances and angles in the structure (packing distance d, H-bond lengths, C1-C4' distance lengths and the angle between the diacetylene rod and the stacking axis ϕ); figure **b** shows the mean planes calculated on two tetrazine rings on two adjacent DA units, which are tilted by 69.2°; figure **c** shows the mean planes calculated on two alkyl chains C12 on two adjacent DA units, which are tilted by 76.98°.

2. Statistical analysis of surface crystal length and orientation (DA1 and TzDA1)

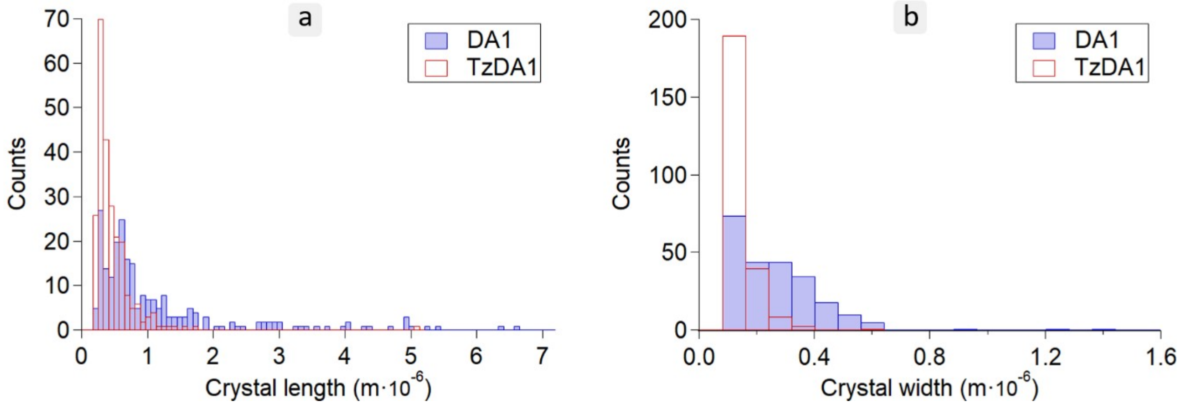

Figure S6. Statistical analysis of surface crystal lengths (a) and widths (b). Blue bars correspond to **DA1** films and red bars to **TzDA1** films. Bin width was set to 80 nm according to AFM images resolution. The analysis was performed on **Figure 2b** for **TzDA1** and on **Figure 2d** for **DA1**.

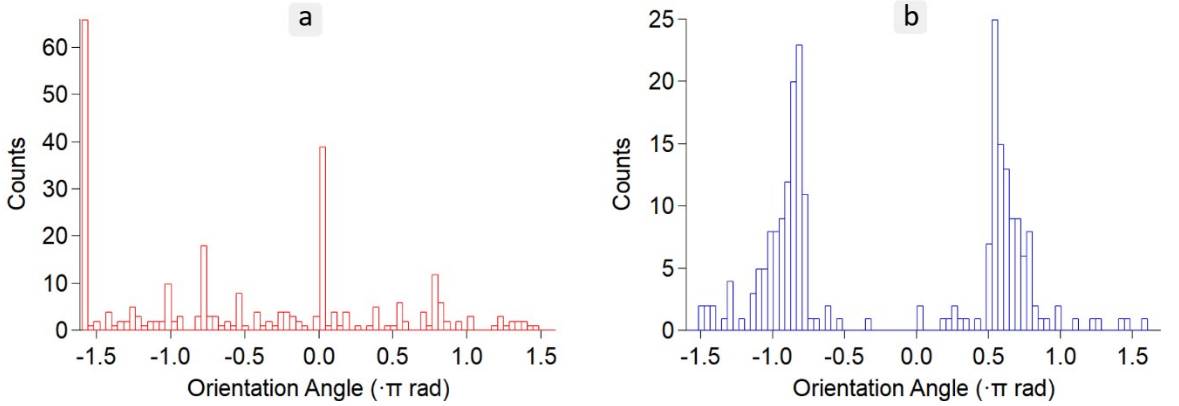

Figure S7. Statistical analysis of surface crystal orientations, showing random orientations in **TzDA1** (a) and two main preferred orientations in **DA1** (b). Bin width was set to 0.04π rad. The analysis was performed on **Figure 2b** for **TzDA1** and on **Figure 2d** for **DA1**.

3. Estimation of Tz-DA film thickness by OD

For an absorbing thin film

$$\alpha = \frac{2.3 \cdot OD}{d} \quad \text{(equation S1)}$$

where ***α*** is the absorptivity of the film, the ***OD*** is the absorbance at the S1 transition of the tetrazine at 530 nm and ***d*** is the thickness of the film. For an 82 nm thick film of **TzDA1** it is found $\alpha = 1.5 \cdot 10^4$ cm^{-1}.

Using this value for **TzDA2** thin film gives a thickness ***d* = 80 nm**.

4. Film thickness measurement by AFM

Film thickness was measured by manually performing a scratch and measuring the step height in 5 different points along the scratch. The obtained mean value is d = 80 ± 12 nm for **TzDA1** and 313 ± 20 nm for **DA1**.

5. Steady-state spectroscopy of DA1

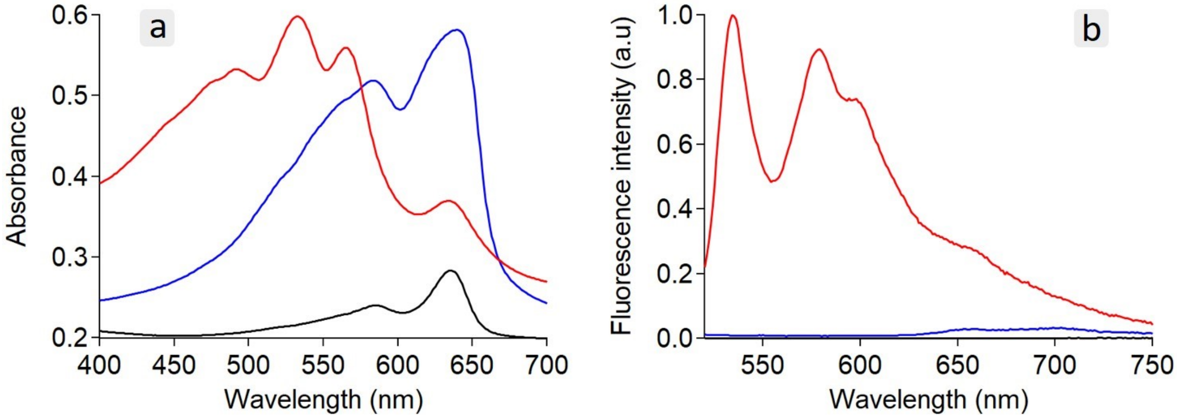

Figure S8. Absorption (a) and fluorescence (b) spectra of **DA1** thin films on quartz slides (λ_{exc} = 488 nm). Black lines correspond to monomeric film, blue lines to polymerized films by 10s irradiation at 254 nm at 3.1 mW·cm^{-2} irradiating power and red lines to heated polymeric films at 80°C on a heating plate.

6. Photophysical properties

6.1. TzDA1 monomer in CH_3CN solution.

For TzDA1, molar extinction coefficient at 520nm (ε_{520} = 650 L mol^{-1} cm^{-1}) and fluorescence quantum yield (0.085) have been described in ref 26 of the main text.

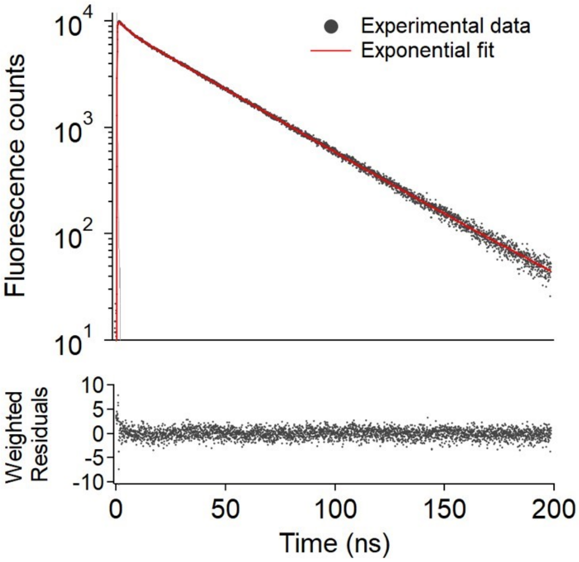

Figure S9. Fluorescence decay profile of **TzDA1** monomer in acetonitrile. λ_{exc} = 495 nm, λ_{em} = 580 nm

The decay is fitted by two discrete exponentials, a short (4.6 ns) and a long one (36.3 ns), the short being less than 1% in the fractional intensity (probably due to some impurity).

6.2. TzDA2 monomer in CH_3CN solution

Fluorescence quantum yields in solution were measured using rhodamine 6G in ethanol (literature Φ_F^R = 95%) as the reference. All solutions were diluted to have an OD < 0.1. The fluorescence quantum yield of the samples Φ_F (x) were calculated using the following equation:

$$\Phi_F(x) = \Phi_F(0) \frac{1-10^{-A_0}}{1-10^{-A_x}} \frac{S_x}{S_0} \left(\frac{n_x}{n_0}\right)^2$$

(equation S2)

with $\Phi_F(0)$ and $\Phi_F(x)$ the fluorescence quantum yield of the reference and of the sample respectively; S_0 and S_x are the integrated fluorescence spectra of the reference and the sample; A_0 and A_x are the values of the absorbance of both samples at the chosen excitation wavelength; n_0 and n_x are the refraction index of the solvent and the solution, respectively. It was obtained $\phi_F = 0.054$ for **TzDA2**

Molar extinction coefficient (ε) was calculated for **TzDA2** monomer at 520 nm in acetonitrile. It was obtained $\varepsilon_{520} = 650$ L mol^{-1} cm^{-1}, which is in good accordance with alkoxy-substituted tetrazines found in literature.[1]

Emission decay curves were measured by an LP920-K spectrometer equipped with a sample holder, a monochromator with 300 mm focus, and a photomultiplier (Hamamatsu R928). The sample was excited at 520 nm by an OPO pumped by an oscillating Nd:YAG nanosecond laser (7-8 ns fwhm at 355 nm) with a repetition rate of 10 Hz. The instrumental response function was recorded with each set of decay curves. The data were analyzed with reconvolution using the L900 software.

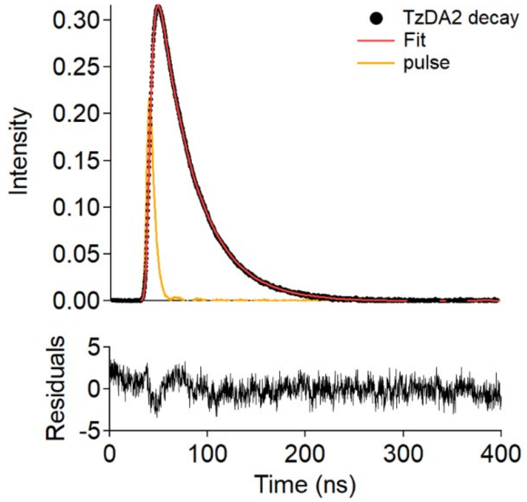

---

[1] Y. H. Gong, F. Miomandre, R. Meallet-Renault, S. Badre, L. Galmiche, J. Tang, P. Audebert and G. Clavier, *Eur. J. Org. Chem.*, 2009, 6121-6128.

Figure S10. Fluorescence decay profile of **TzDA2** monomer in acetonitrile. λ_{exc} = 520 nm, λ_{em} = 560 nm

The decay is fitted by a discrete exponential giving a lifetime of 37 ns.

6.3. Fluorescence lifetime of TzDA2 monomer in thin film

Emission decay curves were measured with a wide-field time-resolved MCP-PMT[2] (LINCam, Photonscore GmbH) coupled to an inverted epifluorescence microscope (TE2000, Nikon®). Global IRF of the TSCSPC is about 60ps (bin width 24ps, 4096 bins). Sample is excited with the SHG of a T-Pulse 200 oscillator (1030nm, 400fs, 10MHz, Amplitude®) at 515nm. Reported decay stands for the full field of view of the detector, 60µm diameter at the sample plane using an X40 NA 0.75 objective.

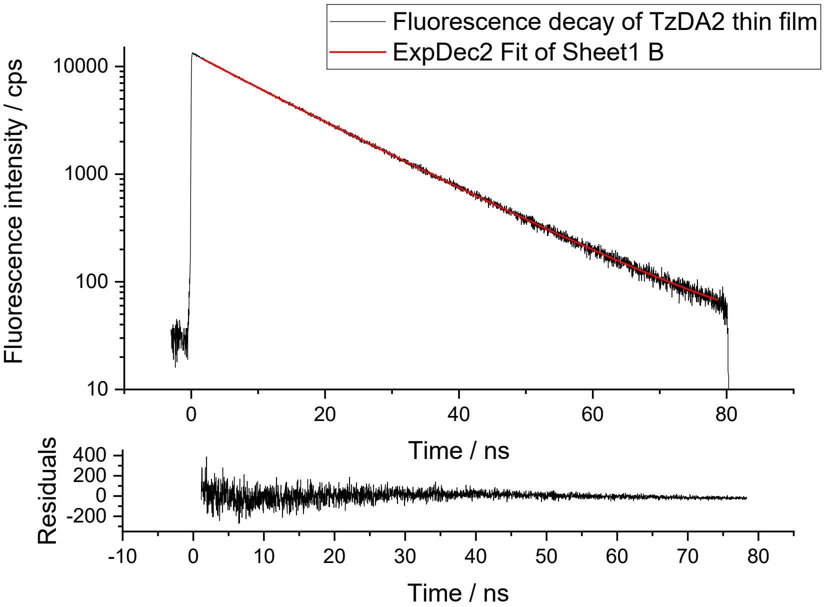

Figure S11. Fluorescence decay profile of a drop-casted film of **TzDA2** monomer on a glass slide. λ_{exc} = 515 nm, λ_{em} = 560 nm

---

[2] Y. Prokazov, E. Turbin, A. Weber, R. Hartig, W. Zuschratter, Position sensitive detector for fluorescence lifetime imaging, *J. Instrum.* 9 (2014) C12015-C12015. https://doi.org/10.1088/1748-0221/9/12/C12015

The decay is fitted by a sum of two discrete exponentials τ1= 8.1ns (a1 = 0.12) and τ2= 14.3ns (a2 = 0.88).

6.4. Solid state fluorescence quantum yields of TzDA2

Solid state fluorescence quantum yields were measured on a drop casted film of **TzDA2**. Before polymerization, it was found ϕ = 0.06; after irradiation at 254 nm (8 min), it was found ϕ = 8.10^{-3}. The drop in fluorescence quantum yield is consistent with an energy transfer mechanism with blue-poly-**TzDA2**, which is the tetrazine quencher.

6.5. Steady-state fluorescence spectra and fitting parameters corresponding to the multi-exponential fits of photopolymerized thin films of TzDA1

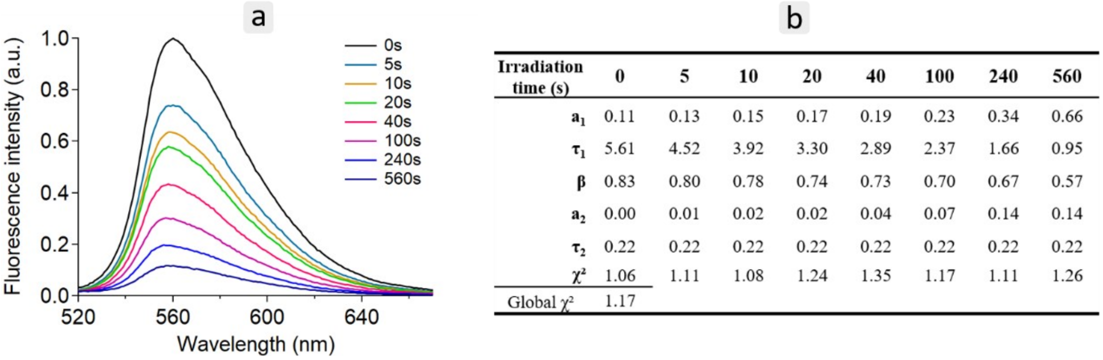

Irradiation time (s)	0	5	10	20	40	100	240	560
a_1	0.11	0.13	0.15	0.17	0.19	0.23	0.34	0.66
τ_1	5.61	4.52	3.92	3.30	2.89	2.37	1.66	0.95
β	0.83	0.80	0.78	0.74	0.73	0.70	0.67	0.57
a_2	0.00	0.01	0.02	0.02	0.04	0.07	0.14	0.14
τ_2	0.22	0.22	0.22	0.22	0.22	0.22	0.22	0.22
χ^2	1.06	1.11	1.08	1.24	1.35	1.17	1.11	1.26
Global χ^2	1.17							

Figure S12. Steady-state fluorescence spectra corresponding to each step of the photopolymerization process (a); table summarizing the fitting parameters of the multi-exponential function for the decay profiles of each step of the photopolymerization process (b)

6.6. Intensity fractions of single components in the multi-exponential fit of photopolymerized thin films of TzDA1.

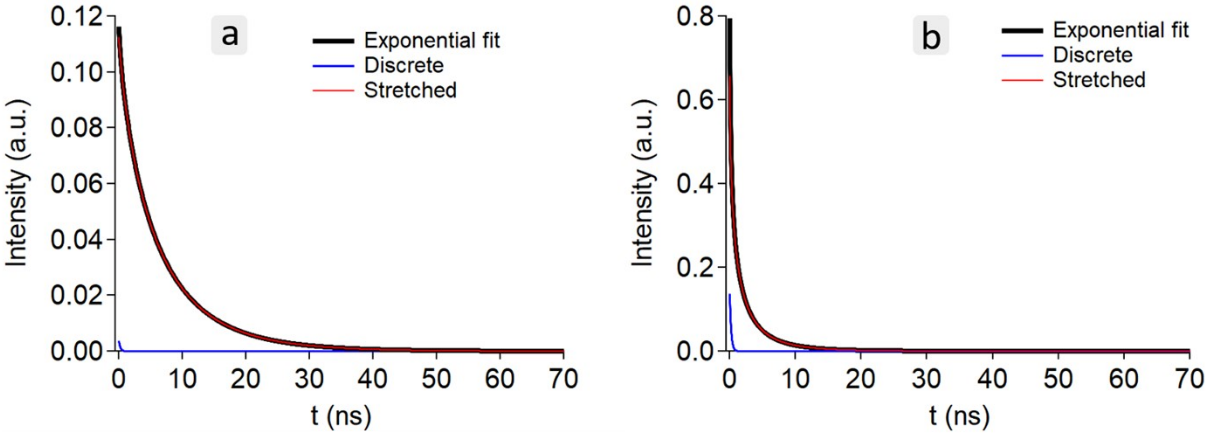

c

Irradiation time (s)	0	5	10	20	40	100	240	560
Fluorescence intensity 560 nm	1.00	0.74	0.63	0.57	0.43	0.30	0.19	0.12
f **discrete**	0.001	0.004	0.007	0.005	0.014	0.023	0.039	0.030
f **stretched**	0.999	0.996	0.993	0.995	0.986	0.977	0.961	0.970
Normalized *f* discrete	0.001	0.003	0.005	0.003	0.006	0.007	0.008	0.003
Normalized *f* stretched	0.999	0.737	0.630	0.571	0.423	0.293	0.185	0.113

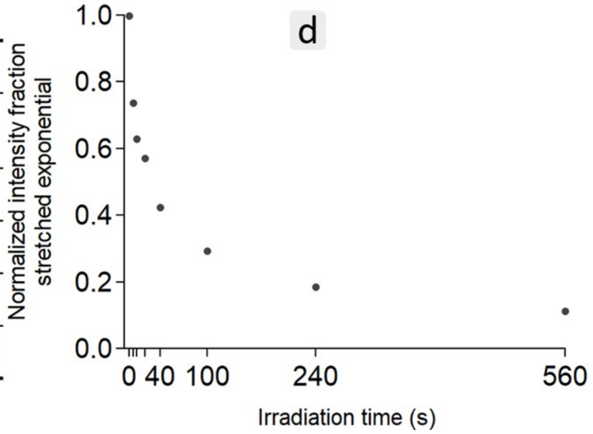

Figure S13. Intensity fractions of single component exponentials of **TzDA1** thin films in the monomer state (a) and irradiated at 254 nm for 560 s (b). The fractions for all stages of polymerization are reported in the table (c) and the normalized intensity fraction of the stretched exponential component is plotted versus the irradiation time (d).

6.7. List of the main photophysical parameters of DA1, TzDA1 and TzDA2

Table S2. List of the main photophysical parameters (maxima of emission, fluorescence quantum yields and fluorescence lifetimes) of acetonitrile solutions and films in the monomeric and polymeric forms (blue/red) of **DA1**, **TzDA1** and **TzDA2**.

	DA1			
	Mono (MeCN)	**Mono (film)**	**Poly (film)**	**Heated**
λ_{em}(max)	No fluo	No fluo	No fluo	534, 579, 598
ϕ_F	No fluo	No fluo	< 1%	< 1%
τ	No fluo	No fluo	No fluo	< 10 ps[a]
	TzDA1			
	Mono (MeCN)	**Mono (film)**	**Poly (film)**	**Heated**
λ_{em}(max)	568	560	557 (glass); 570 (paper)	560
ϕ_F	8.50%	17.30%	1.20%	10.50%
τ	36 ns[a]	τ1= 5.61 ns (a1 = 0.11, β = 0.83) [a]	τ1= 0.95 ns (a1 = 0.66, β = 0.57) τ2= 0.22 ns (a2 = 0.14) [a]	<⍰> = 10.4 ns[a]
	TzDA2			
	Mono (MeCN)	**Mono (film)**	**Poly (film)**	**Heated**
λ_{em}(max)	569	563	563 (glass); 570 (paper)	565 (glass)
ϕ_F	5.40%	6.00%	0.80%	1.50%
τ	37 ns[c]	τ1 = 8.1 ns (a1 = 0.12) and τ2 = 14.3 ns (a2 = 0.88)[b]	<5ns[c]	9ns[c]

[a] Excitation was done via Titanium:Sapphire femtosecond oscillator laser (Tsunami, Spectra Physics) pumped by a double intra-cavity Nd:YVO4 laser (Millenia Xs, Spectra Physics). The wavelength was adjusted at 720 nm at the output of the oscillator. Repetition rate was reduced to 4 MHz by a pulse selector (model 3980, Spectra Physics). The wavelength at 360 nm was generated by focalizing the fundamental beam at 720 nm inside a nonlinear SHG crystal. The pulse duration of the excitation laser at 360 nm was less than 500 fs. The emission was detected perpendicular to the excitation beam through a low pass filter (to remove the excitation light), an analyzer at magic angle, a monochromator, and a MCP-PMT detector (R3809U-50, Hamamatsu) connected to a TCSPC card (SPC 630, Becker & Hickl). The instrumental response function was recorded for each decay curve. The data were analyzed with multiexponential functions including reconvolution analysis, using the Globals software (Laboratory for Fluorescence Dynamics at the University of California, Irvine).

[b] Emission decay curves were measured with a wide-field time-resolved MCP-PMT[3] (LINCam, Photonscore GmbH) coupled to an inverted epifluorescence microscope (TE2000, Nikon®). Global IRF of

the TSCSPC is about 60ps (bin width 24ps, 4096 bins). Sample is excited with the SHG of a T-Pulse 200 oscillator (1030nm, 400fs, 10MHz, Amplitude®) at 515nm. Reported decay stands for the full field of view of the detector, 60µm diameter at the sample plane using an X40 NA 0.75 objective.

[c] Emission decay curves were measured by an LP920-K spectrometer equipped with a sample holder, a monochromator with 300 mm focus, and a photomultiplier (Hamamatsu R928). The sample was excited at 355 or 520 nm by an OPO pumped by an oscillating Nd:YAG nanosecond laser (7-8 ns fwhm at 355 nm) with a repetition rate of 10 Hz. The instrumental response function was recorded with each set of decay curves. The data were analyzed with reconvolution using the L900 software.

7. Macroscale mechanofluorochromism of DA1 and TzDA1

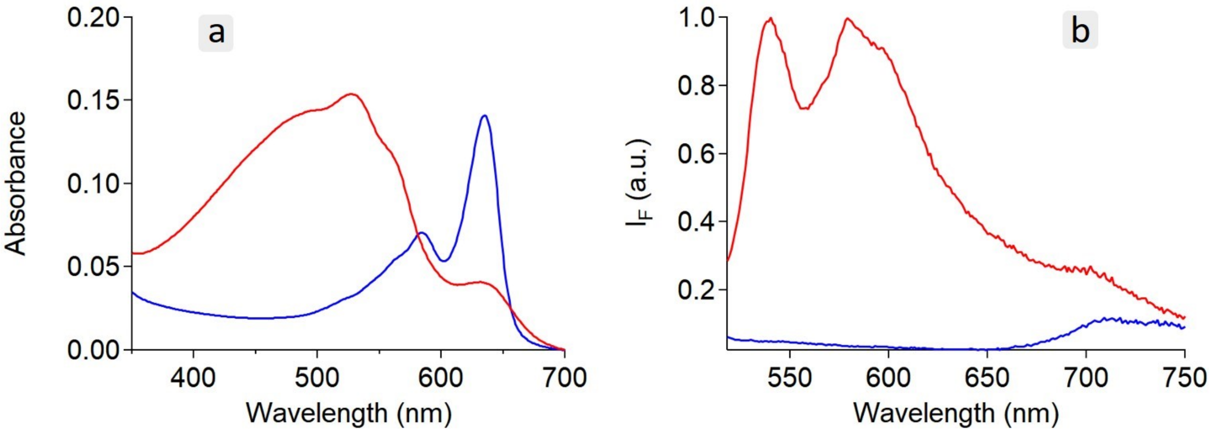

Figure S14. Absorption spectra of UV-polymerized **DA1** vacuum evaporated thin film (blue line) and of red-poly-**DA1** obtained by rubbing on the substrate (red line) (a); fluorescence spectra of blue- (blue line) and red- (red line) poly-**DA1** (b).

---

[3] Y. Prokazov, E. Turbin, A. Weber, R. Hartig, W. Zuschratter, Position sensitive detector for fluorescence lifetime imaging, *J. Instrum.* 9 (2014) C12015-C12015. https://doi.org/10.1088/1748-0221/9/12/C12015

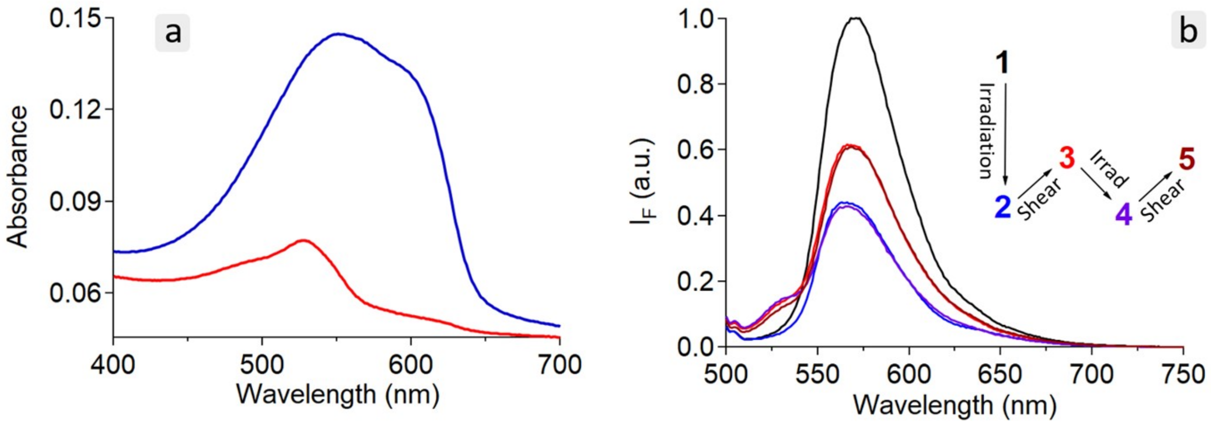

Figure S15. Absorption spectra of a vacuum evaporated thin film of **TzDA1** before (blue) and after (red) mechanical rubbing with a spatula (a); fluorescence spectra of a film on paper before polymerisation (black), and after two consecutive cycles of irradiation (blue, purple)/shearing (red, brown) (b). (figure modified from reference 26 of main text). On figure S15b, integrating the area of the fluorescence spectra of the monomeric, polymeric and stimulated film allows to calculate a percentage of fluorescence recovery equal to $[I_F(\text{sheared})-I_F(\text{poly})]/I_F(\text{mono})$ = 21%,

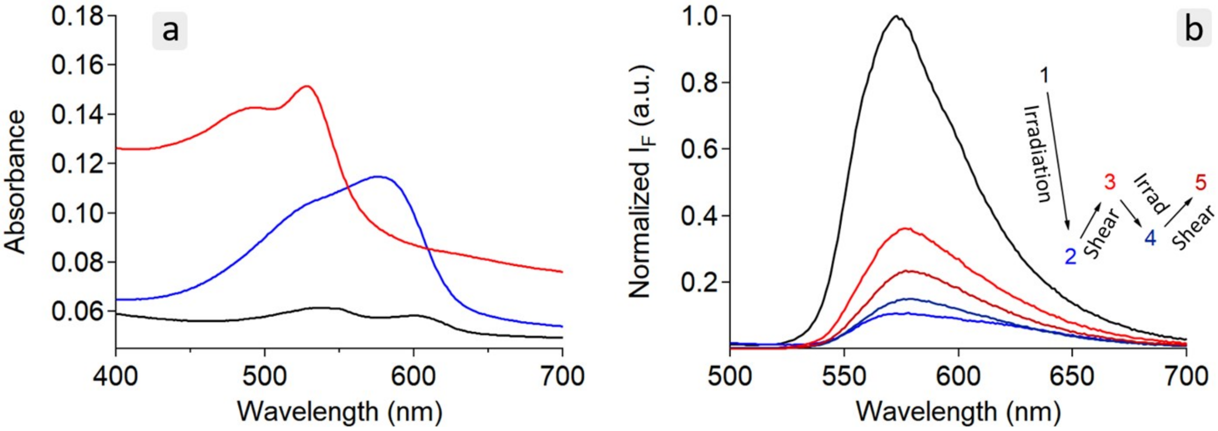

Figure S16. Absorption spectra of a vacuum evaporated thin film of **TzDA2** before polymerization (black), before (blue) and after (red) mechanical rubbing with a spatula (a); fluorescence spectra of a film on paper before polymerisation (black), and after two consecutive cycles of irradiation (blue, purple)/shearing (red, brown) (b).

7.1. Macroscale mechanofluorochromism of TzDA1 deposited by spin-coating on different supports

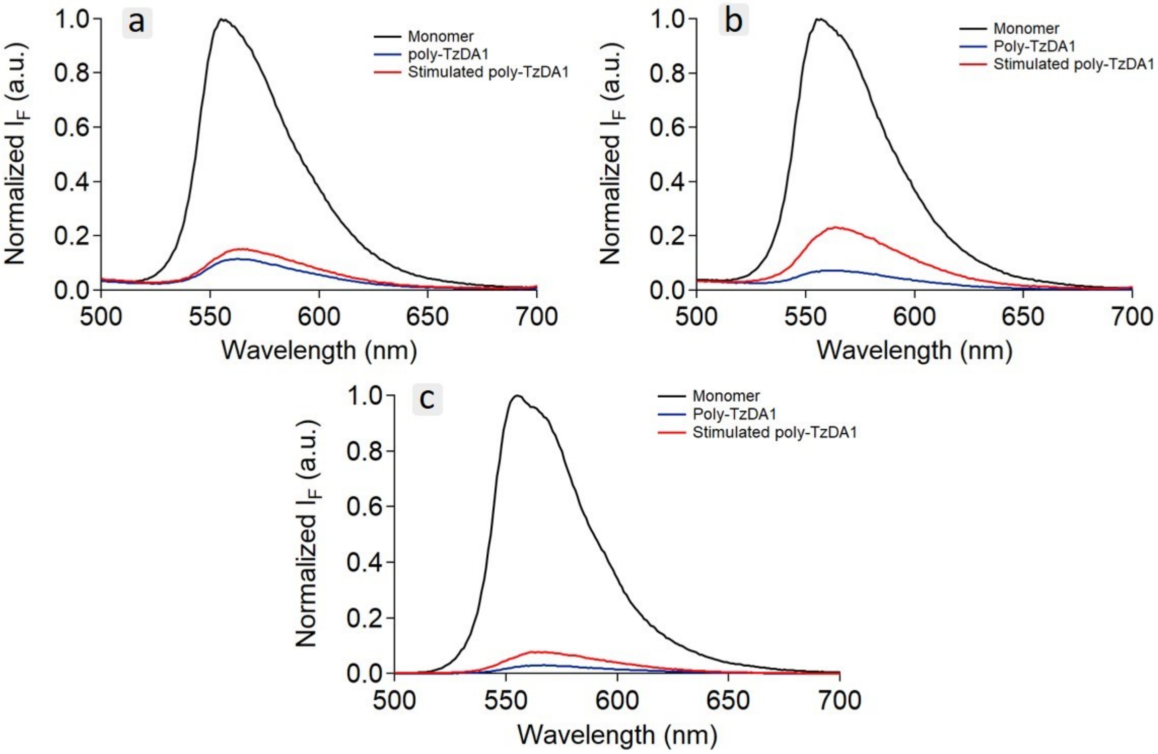

Figure S17. Fluorescence spectra before irradiation (black lines), after irradiation (blue lines) and after macroscale mechanical stimulation (red lines) of TzDA1 spin coated on a glass slide (a), ITO (b) and silicon (c).

Spin coating parameters Glass: 2000 rpm, 2 min; ITO: 1000 rpm, 2 min; Silicon: 1000 rpm, 2 min

8. Microscopy

8.1. High forces on DA1

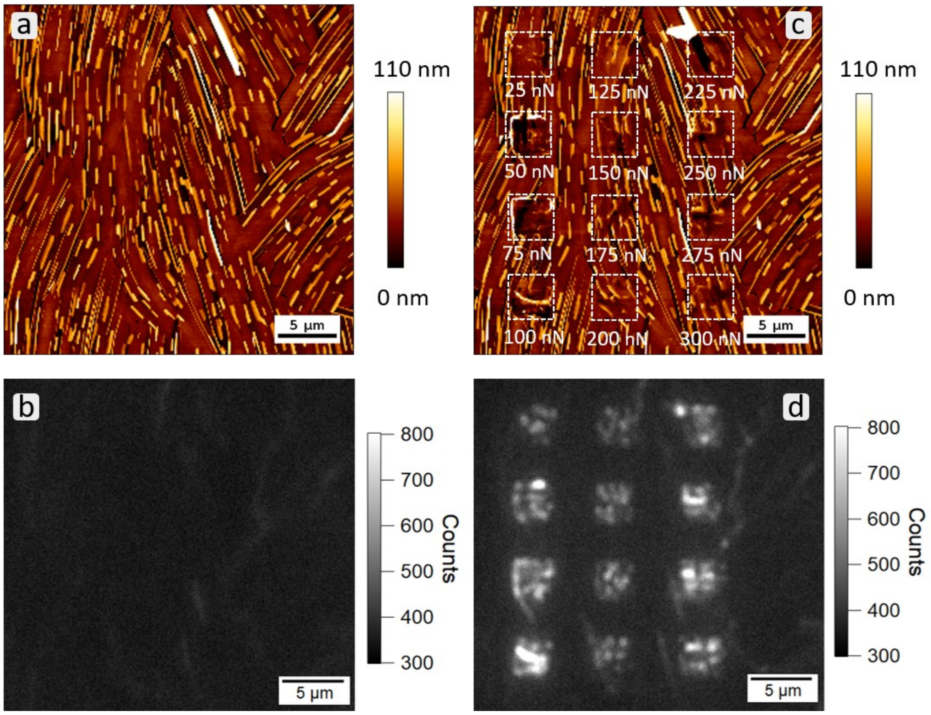

Figure S18. Morphology and corresponding fluorescence images (λ_{exc} = 488 nm) of **DA1** thin films before (a, b) and after (c, d) mechanical stimulation. Each area was scanned from bottom to top with forces ranging from 325 to 600 nN at a tip velocity of 6.1 µm·s^{-1}.

8.2. Experiments on TzDA2

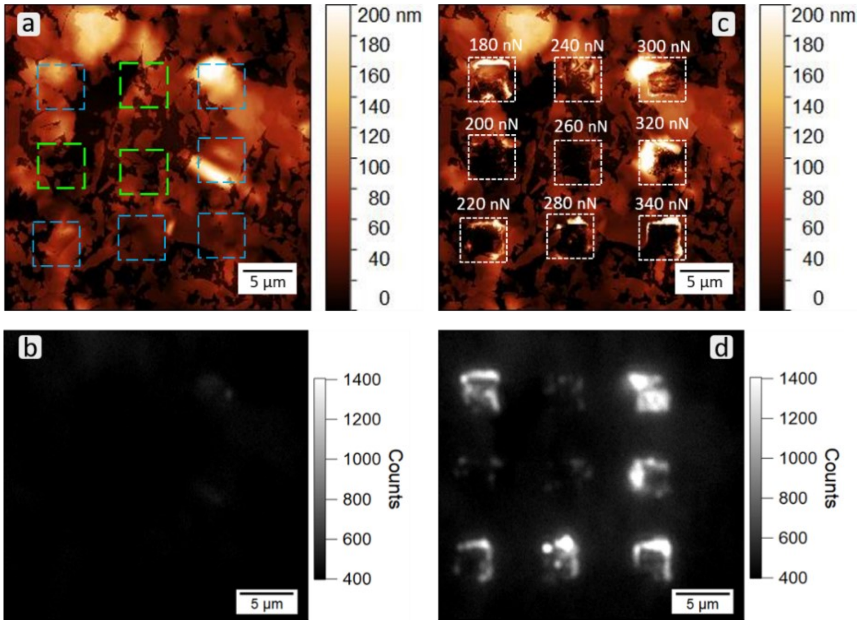

Figure S19. Morphology and corresponding fluorescence images (λ_{exc} = 488 nm) of **TzDA2** thin films before (a, b) and after (c, d) mechanical stimulation. Each area was scanned from bottom to top with forces ranging from 180 to 340 nN at a tip velocity of 6.1 µm·s^{-1}.

8.3. List of mechanical stimulations on DA1 and TzDA1

Table S3. Number of mechanical stimulations performed on different zones of the same **DA1** thin film. For each applied force, the mean fluorescence signal and the standard deviation is also specified.

Force (nN)	Number of measurements	Mean fluorescence signal	Standard deviation
20	1	19905	-
25	2	39161	36331
40	1	3824	-
50	6	35153	45880
60	1	10101	-
75	2	92928	100493
80	1	22795	-
100	7	47584	74464
120	1	8060	-
125	2	38562	19092
140	1	18701	-
150	6	39169	24055
160	1	27032	-
175	2	55867	36056
180	1	10287	-
200	7	80135	86515
225	2	74927	42885
250	8	68762	39954
275	2	100638	78735
300	6	69194	33813
325	2	60060	14661
350	7	59185	20966
375	3	41534	6796
400	7	67557	23458
425	2	177866	174091
450	5	83286	42482
475	2	108020	56117
500	6	77338	28849
525	2	60570	11640
550	5	57494	24331
575	1	88766	-
600	3	103107	32451

Table S4. Number of mechanical stimulations performed on different zones of the same **TzDA1** thin film. For each applied force, the mean fluorescence signal and the standard deviation is also specified.

Force (nN)	Number of measurements	Mean fluorescence signal	Standard deviation
20	5	114370	70493
40	6	280882	84885
50	1	273365	-
60	6	359497	203645
80	7	404576	180686
100	6	448397	229488
110	1	274354	-
120	6	467896	209876
140	7	580273	294664
160	6	606225	127161
170	1	798482	-
180	6	581151	152310
200	8	659717	111323
220	6	663174	117240
230	1	658357	-
240	6	658715	109659
250	1	527456	-
260	7	611385	233222
280	6	652292	38701
290	1	663964	-
300	5	570738	141160
310	1	597822	-
320	1	598586	-
340	2	551132	192258
350	1	596151	-
360	1	609874	-
370	1	618559	-
380	1	535611	-
400	3	629372	15714
430	1	633493	-
450	1	500366	-
460	1	546056	-
500	1	536697	-

8.4. Application of a vertical force on TzDA1 thin films

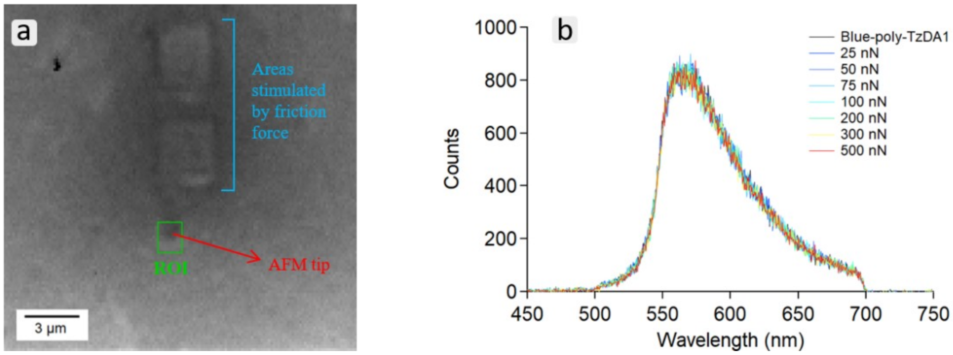

Figure S20. Application of a vertical force by AFM on a thin film of **TzDA1**. Image of the sample area (a), where the green square shows the ROI of the acquired fluorescence spectra and the red arrow points at the position of the AFM tip. Fluorescence spectra of consecutive vertical force applications from 25 to 500 nN (b).

Applying only the vertical force does not cause any variation in the fluorescence signal. The AFM tip is placed on the film and consecutive vertical forces from 25 to 500 nN are applied. A fluorescence spectrum is acquired over the ROI (region of interest) shown in Figure a by the green square after each force application. The spectra are shown in Figure S15b, and they all overlap with the spectrum acquired in the same zone before mechanical stimulation.

8.5. Deposition of TzDA1 by spin coating on other substrates

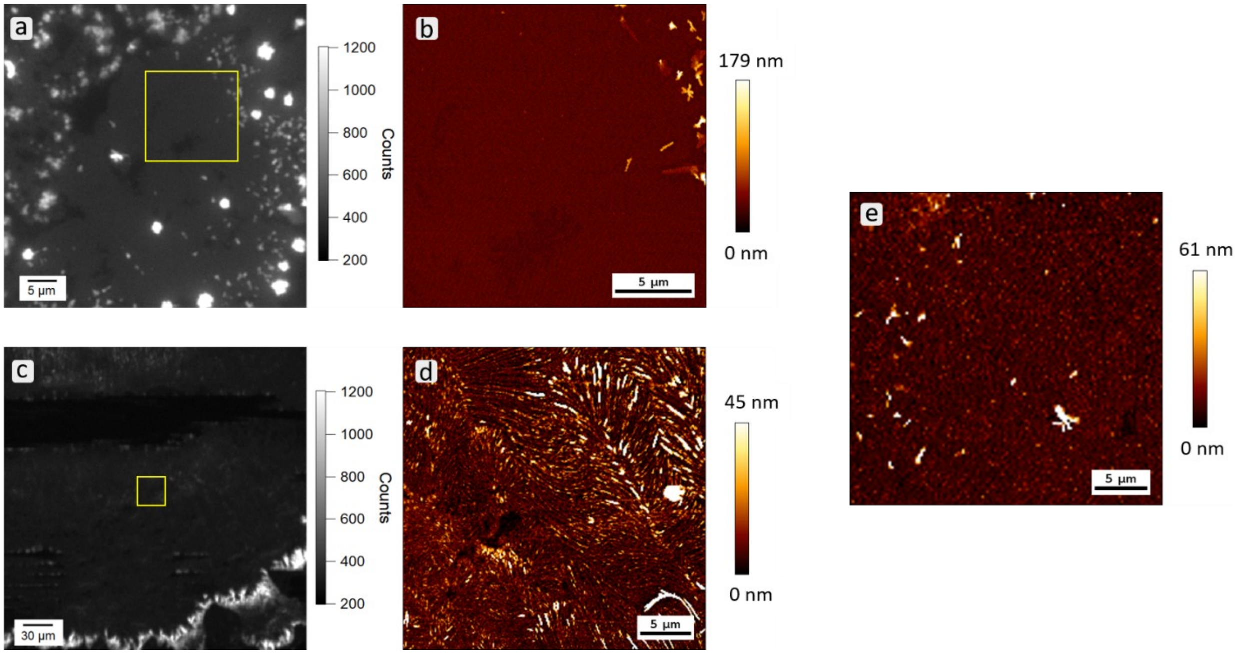

Figure S21. Fluorescence and topography images of spin coated films of a 0.5 mM solution of **TzDA1** in MeCN on different substrates at 1000 rpm for 2 min. Fluorescence (a) and topography (b) images of spin coated **TzDA1** on glass substrate; fluorescence (c) and topography (d) images of spin coated **TzDA1** on ITO substrate; topography image of spin coated **TzDA1** on silicon wafer (e). Fluorescence images are recorded at λ_{exc} 488 nm with 1 s integration time.

8.6. Estimation of the fluorescence recovery level for TzDA1 at the nanoscale

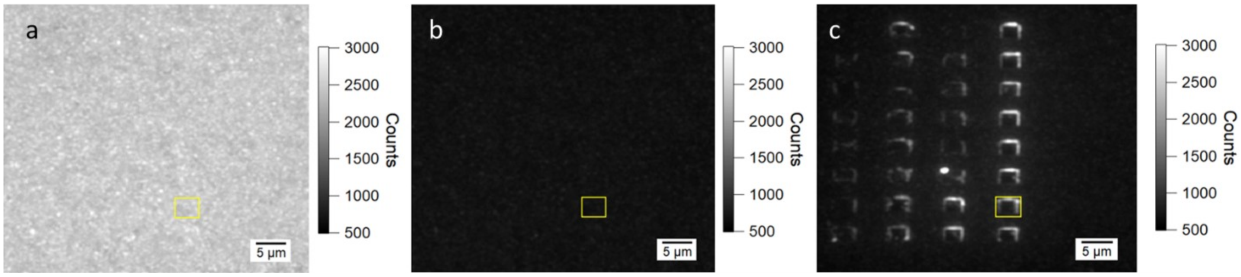

Figure S22. Fluorescence images of vacuum evaporated thin film of **TzDA1** on glass as evaporated (a), after photopolymerization (b), after mechanical stimulation (c). Integration of the fluorescence intensity level is made on a 30x40 pixels (yellow rectangle) on the three pictures which allows to measure a fluorescence recovery percentage equal to $[I_F(\text{sheared})-I_F(\text{poly})]/I_F(\text{mono}) = 27\%$. λ_{exc} 488 nm, 1 s integration time.